What is Open Access?
Open Access is an initiative that aims to make scientific research freely availabl
of collaboration, unobstructed discovery, and, most importantly, scientific pro
decided to create a new Open Access publisher that levels the playing field for s
needs of the researchers before the business interests of publishers.
Our authors and editors
We are a community of more than 103,000 authors and editors from 3,291 insti
cited researchers. Publishing on IntechOpen allows authors to earn citations an
study, but from other related fields too.
Content Alerts
Brief introduction to this section that descibes Open Access especially from an

Distributed Smart Sensing Systems for In

By Octavian Postolache, Jose Migue

Submitted: October 16th 2010 Revie

DOI:

Home > Books > Chemistry, Emission Control, Radioactive Pollution and Indoor Air Quality

1. Introduction

Indoor air quality pollution [ ][2] represents one of the factors associated with the etiology of chronic obstructive pulmonary disease and also plays an important role in respiratory distress, the second most common symptom of adults that request emergency transportation to the hospital and is associated with a relatively high overall mortality before hospital discharge [ ][ ][ ][ ]. The prevention of acute respiratory distress or asthma attacks can be possible by monitoring the air quality conditions using distributed smart sensing systems characterized by accuracy, short time response, and robustness as well as by data processing, data logging and data communication capabilities.

Considering the importance of indoor air quality monitoring, different distributed measuring system architectures and associated calibration methods and systems are presented in the literature [ ][ ][ ]. The main elements of these kind of systems are not only temperature and relative humidity sensors, but also gas detectors and gas concentration sensors whose metrological characteristics, such as accuracy and linearity are very limited, which implies the design and implementation of signal processing algorithms namely for numerical linearization and common factors correction [ ][ ][ ].

Taking into account the indoor spatial distribution of the temperature and relative humidity values as well as the concentration values of pollutants (e.g CO, CO_2 resulting of combustion), the development of distributed measuring syst[illegible] that can include personal computers (PCs) or mobile devices (e.g. PDAs [ ] or smart phones [ ]) based human-sensing system interface represents

This chapter presents a practical approach concerning distributed smar the authors in this area. The first part of the chapter deals with the relat conditions. The second part contains a brief presentation of solid state s the third part presents a distributed architecture based on an embedded fourth part, a Bluetooth wireless distributed system including smart sen monitoring system interfacing device is presented.

Referring to the distributed air quality monitoring system based on emb oxide semi-conductor sensor array that includes general air contaminan pollution alarms from the nodes, which are parts of a wired or wireless temperature and relative humidity sensors are included in the node's ha and humidity influences. This chapter also includes a brief description used to obtain temperature and humidity compensated gas concentratic designed and implemented for continuous monitoring of indoor humid

the chapter. Bluetooth compatible nodes, characterized by data acquisiti
using Java2ME to perform different tasks including data communicatior
indoor air quality monitoring system. Elements regarding the smart phc
architecture and air quality monitoring tasks are discussed and an exam
system, an intelligent assessment of air conditions for risk factor reduct

2. Air quality and its impact on respiratory diseases

Air conditions and respiratory assessment represent an important challenge taking into account that distress is the second most common symptom of adults transported by ambulance and is associated with a relatively high overall mortality before hospital discharge [ ]. Among the most common causes of respiratory distress in this setting are congestive heart failure, pneumonia, chronic obstructive pulmonary disease and asthma [ ]. It is projected that chronic obstructive pulmonary disease (COPD) will be the third leading cause of death worldwide by 2020, due to an increase in smoking rates and demographic changes in many countries [ ]. Worldwide, some 300 million people currently suffer from asthma. It is the most common chronic disease among children [ ]. The economic burden of COPD in the US in 2007 was 42.6 billion in health care costs and lost productivity [ ]. The indoor air pollution is one of the factors associated with etiology of chronic obstructive pulmonary disease and asthma. There are evidences that the environmental factors acting during early life and interacting with specific "asthma genes" are crucial for the development of chronic, persistent form of disease [ ][ ]. The identification of the indoor air associated with pathophysiology of COPD and asthma disease will thus be crucial for the primary-prevention strategy.

Poor indoor air quality is becoming an increasing problem around the world because, in general, people are spending more time indoors. This problem is greater in infants who now spend less time playing outside. Reduction of indoor air quality - produced by mould growth, smoke exposure, cooking fire smoke (often using biomass fuels such as wood and animal dung), house dust mites in bedding, carpets and stuffed furniture, chemical irritants (i.e. perfumes), pet dander – may adversely affect the health of building occupants and exacerbate asthma and COPD attacks. Asthma attacks are mainly related to mould growth that is enabled by relative humidity high values for different temperature conditions. Mould spores, bacteria, and mildew thrive in dampened towels, washcloths, and moist or humid areas. Additionally, people with immune or respiratory system problems may more easily succumb to poor health caused by mould growth at home, which is mainly associated with humidity and temperature values. Improved heating systems and less ventilation from outside has also provided more suitable conditions for mould growth. Using air conditions sensing components as parts of an air quality measuring system, high risk disease conditions for indoor occupants can be avoided. Several solutions have been presented in the literature [ ][ ][ ]. In order to assure mobility and flexibility, a wireless network for air quality is an interesting solution considering that the measuring
monitoring scenarios. As the interface between a user and the network
enabled), a PDA (personal digital assistant), or situated displays with ir

3. Air quality sensing and data processing

This section contains the description of the main components of a distri
attention is dedicated to the implementation of the sensing nodes, to sig

A. Sensing nodes

The sensing nodes are designed and implemented to perform the air quality (AirQ) monitoring using low cost gas sensors and, at the same time, to get additional information about the temperature (T) and relative humidity (RH). This information is used to increase gas concentration measurement accuracy, performing the error compensation caused by temperature and humidity influence.

The gas sensors can be sintered SnO_2 semiconductor heated sensors, as those provided by Figaro [ ], that assure pollution event detection (TGS800 – general air contaminant sensor - AC), methane detection (TGS842-M), alcohol and organic solvent detection (TGS822-SV) and carbon monoxide detection (TGS203-CO). Information about temperature and relative humidity are obtained using Smartec SMT160-30 [ ] and Humirel HM1500 [ ] temperature and relative humidity transducers, respectively.

The gas sensors, connected to proper conditioning circuits, are devices that produce voltages whose values depend on the concentrations of gas expressed in ppm. The used conditioning circuit for the air pollution sensor TGS800, solvent vapors (TGS822) and methane sensor (TGS842) are presented in .

Electrochemical cells can also be used to implement the sensing units. The NAP-505 [ ] is a typical example of this kind of implementation. In this cased, the 3 terminals measuring cell consists of 3 porous noble metal electrodes separated by an acidic aqueous electrolyte, housed within a plastic enclosure. The working principle of the sensing unit is based on chemical reactions between gas and other elements. From the electrical charges that are involved in those reactions it is possible to measure an electrical current that is proportional to gas concentration. Using multiple cells it is possible to measure the concentration of different gas types.

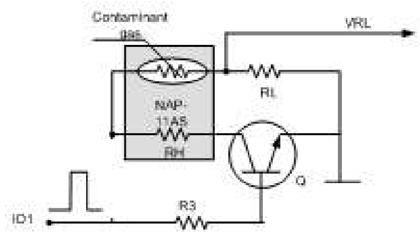

Figure 1.

Gas sensing unit based on semiconductor hea
VGS – gas sensor output voltage, RL – load re

represents the main elements of a gas sensing unit based on an

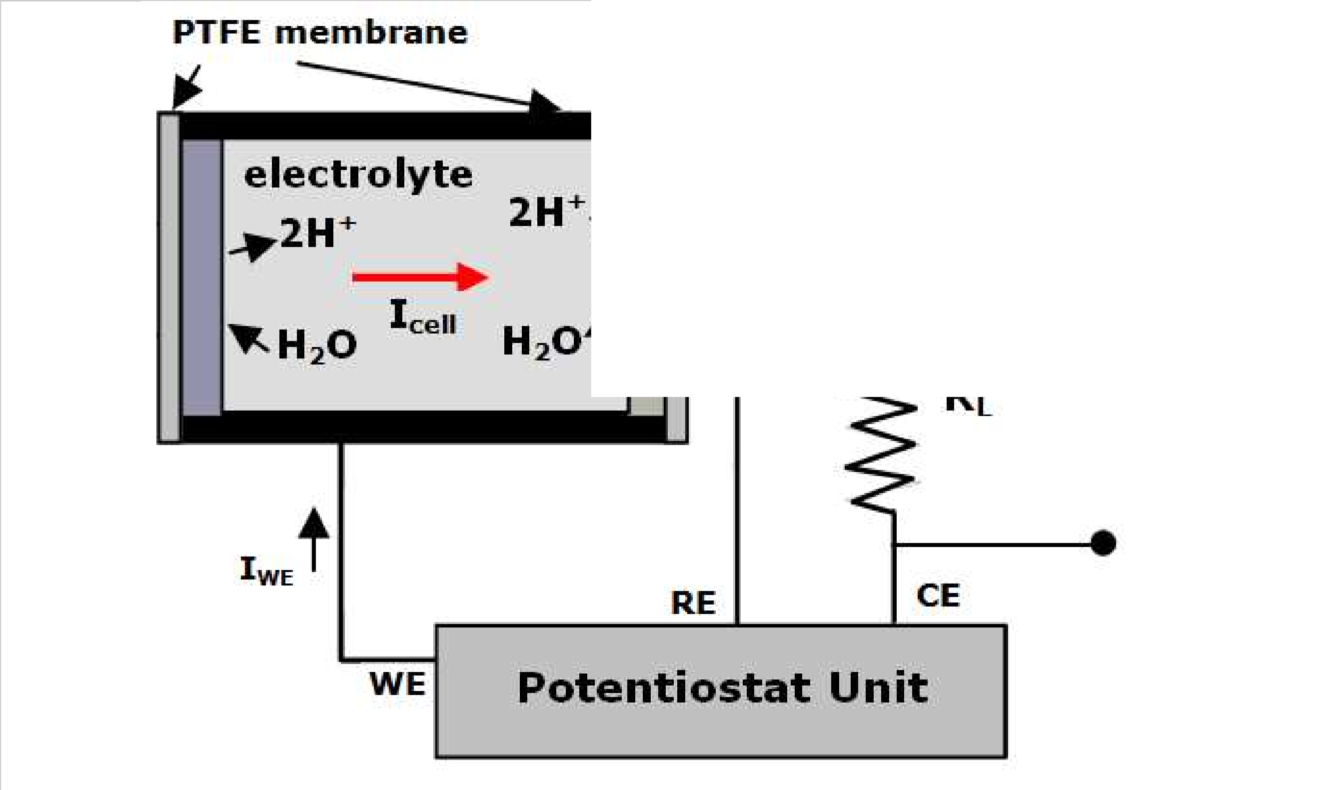

Figure 2.

Gas sensing unit based on an electrochemical cell (RE - reference electrode, CE - counting electrode, WE - working electrode, RL – load resistance)

The measuring cell includes a working electrode (WE), a counter electrode (CE) and a reference electrode (RE) [ ]. The conditioning circuit is basically a potentiostat unit that measures the gas dependent current amplitude (I_{cell}) that flows between the CE and WE through cell's electrolyte. The current amplitude is directly proportional to the gas concentration but its value is usually very low, about a few tens of nA. For this reason a careful design of the potentiostat is crucial to obtain an acceptable measurement. represents the electrical diagram of a typical potentiostat conditioning circuit [ ][ ]. The negative feedback loop, provided by operational amplifiers (OA1 and OA2) and the electrical connection that exists between CE and RE electrodes through the sensing element, assures that the operational amplifiers are working in their linear zones. Since the current between the working and the reference electrodes is very low, the differential voltage between working and counter electrodes is equal to VRE and the output voltage (VADC) from the current to voltage converter implemented by sub-circuit 2 is given by

$$V_{ADC} = -R_F \cdot [f_{sol.}(V_{DAC}) - I_B]$$

E1

where RF represents the feedback resistor of the current to voltage converter, IB represents the polarization current of OA2, VDAC is the output voltage of the D/A converter and fsol is generally a non-linear function that depends on solution characteristics and applied voltage (VWE).

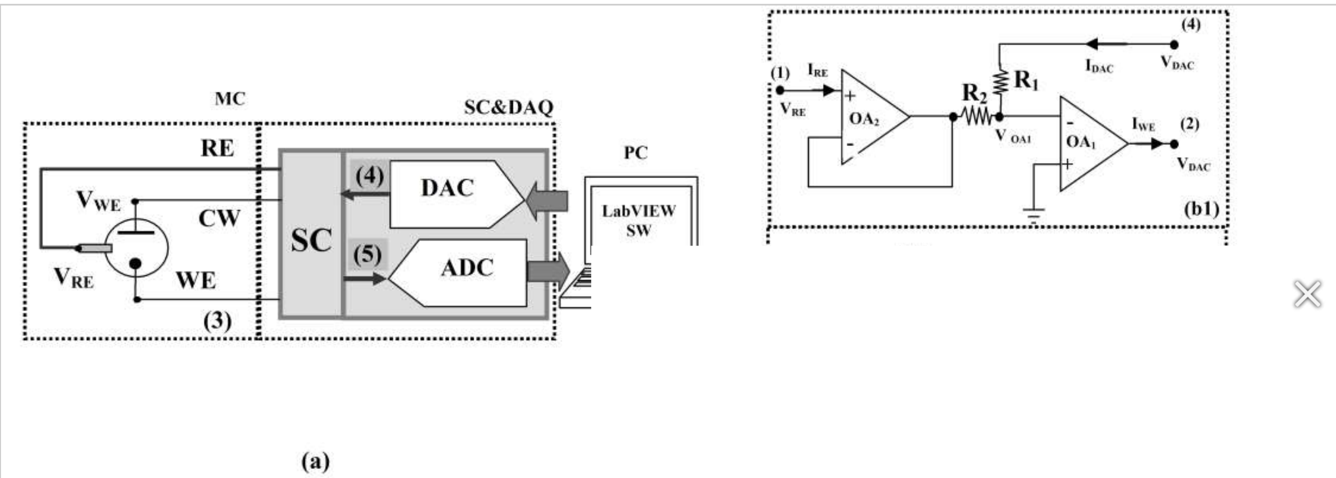

Figure 3.

Electrical circuit of a voltammetry measurin

CE- counting electrode, WE- working electr

ADC- analogue to digital converter, DAC- di

Another attractive solution that can be used to implement the sensing n
interdigitated transducer etched onto a piezoelectric substrate, covered
chemical substance from the air. This causes a shift in resonance to a sli

---

B. Measurement data interpolation

To perform the interpolation of the calibration data in order to obtain th
namely, polynomial interpolation and artificial neural networks (ANNs

Assuming, for simplicity, a single variable function (f) and a LMS polyn

$$P_n(x) = \sum_{k=0} \alpha_k \cdot x^k$$

E2

where p represents the degree of the polynomial curve fitting function and x represents the independent variable - measured quantity - it is possible to demonstrate that the LMS deviation between calibration and curve fitting data is obtained when the coefficients of the curve fitting polynomial function are given by

$$[\alpha] = \left[X_C^T \cdot X_C\right]^{-1} \cdot \left[X_C^T \cdot Y\right]$$

E3

being vector Y and matrix X_C defined, for a set or n calibration points, by

$$Y = \begin{bmatrix} y_1 \\ y_2 \\ \vdots \\ y_n \end{bmatrix} X_C = \begin{bmatrix} 1 & x_1 & x_1^2 & \ldots & x_1^p \\ 1 & x_2 & x_2^2 & \ldots & x_2^p \\ \vdots & \vdots & \vdots & \ldots & \vdots \\ 1 & x_n & x_n^2 & \ldots & x_n^p \end{bmatrix}$$

E4

The concerns related with polynomial interpolation are mainly associated with the choice of the polynomial degree. If a low polynomial degree is used, the interpolation error is generally high because the polynomial function can not fit correctly a large number of calibration points. Conversely, if an excessive polynomial degree is used, the LMS deviation between calibration data and the values obtained from the polynomial interpolation function may be very low, but the interpolation errors of points between calibration data are usually very high. This problem is usually known as overfitting and the previous one as underfitting.

Regarding ANN [ ][ ][ ], the curve fitting function can be computed using the following expression:

$$F_{ANN}(x_i) = F_N\left(W_N^*\left(F_{N-1}\left(\ldots F_2\left(W_2^*F_1\left(W_1^*x_i + B_1\right) + B_2\right)\ldots + B_{N-1}\right) + B_N\right)$$

E5

where N represents the number of neural network (NN) layers, Bi the bias vectors, Wi the weight vectors and Fi the activation transfer function of each layer.

The most common ANN structure for measurement applications contains a hidden layer of neurons with sigmoidal activation functions whose input is the measured data, and an output layer of neurons with linear activation functions. This ANN structure calculates an output vector given by

$$F_{ANN}(x_i) = \text{purelin}\left(W_2^*\text{tansig}\left(W_1^*x_i + B_1\right) + B_2\right)$$

E6

where purelin() and tansig() are linear and hyperbolic tangent sigmoidal activation transfer functions, respectively.

This architecture has proved capable of approximating any function with a finite number of discontinuities and with arbitrary accuracy. Generally a more complex function, such as transducer characteristics that are strongly non-linear, requires more sigmoidal neurons in the hidden layer.

To evaluate the capability of a given solution to generalize the learned fu
correspondent interpolated errors are evaluated. The best values of [B] a
by minimizing the mean square error

$$MSE(x)$$

E7

Several gradient methods [ ][ ], like back propagation (generalized Δ
set of input values corresponding to the calibration points is used to adj
output and the calibration values.

Even if there is no general rule to choose polynomial or ANN based cur
are available, and especially when extrapolation capabilities are desired,

particularly true for non-linear and non-deterministic sensors' characte
terms of the computational load caused by an higher number of mathen
(tanh()) [ ][ ][ ][ ].

C. Data processing: an application example

In order to take advantage of the joint use of polynomial and artificial neural network (ANN) curve fitting techniques [ ][ ], this section describes a hybrid solution based on polynomial modelling (PM) and artificial neural networks modelling (ANN-M) that can be used to estimate the values of air quality parameters, such as, temperature, relative humidity, and polluting gases concentration.

For the particular case of broadband gas sensors, different methods can be used to convert the measured data into concentration of possible gas contaminants, such as, methane, carbon monoxide, isobutane, hydrogen, ethanol or cigarette smoke. Considering the voltage generated by a gas sensing unit based on a semiconductor heated sensor (TGS800 from Figaro), an air quality index ζ, is defined using the following relation

$$\zeta = \frac{R_S}{R_{S0}} = \left(\frac{V_C}{V_{RL}} - 1\right) \cdot \frac{1}{\left(\frac{V_C}{V_{RL0}} - 1\right)}$$

E8

where R_{S0} represents the sensor resistance for a clean air condition, R_S represents the sensor resistance for the tested air, V_C is the circuit power supply voltage, V_{RL} is the load resistor voltage and V_{RL0} is the load resistor voltage for clean air.

Sensor's characteristic is non-linear and monotonic, decreasing sensor's resistance ratio with contaminant gas concentration. Higher concentrations of contaminants originate lower values of resistance ratios. Moreover, since the sensor is designed for general contaminants detection, it is not possible to identify specific contaminants. So, according to the application requirements in terms of the maximum acceptable level of contamination, a coefficient (ζ) value equal to 0.3 is considered for air pollution alarm. Considering that the used sensor has not good selectivity for each potential air contaminant, a look-up table, a polynomial, and a multilayer perceptron single-input single output neural network were designed and implemented to convert the value of ζ into air contaminants' concentrations expressed in parts per million (ppm). The measurement data processing scheme that was implemented is represented in .

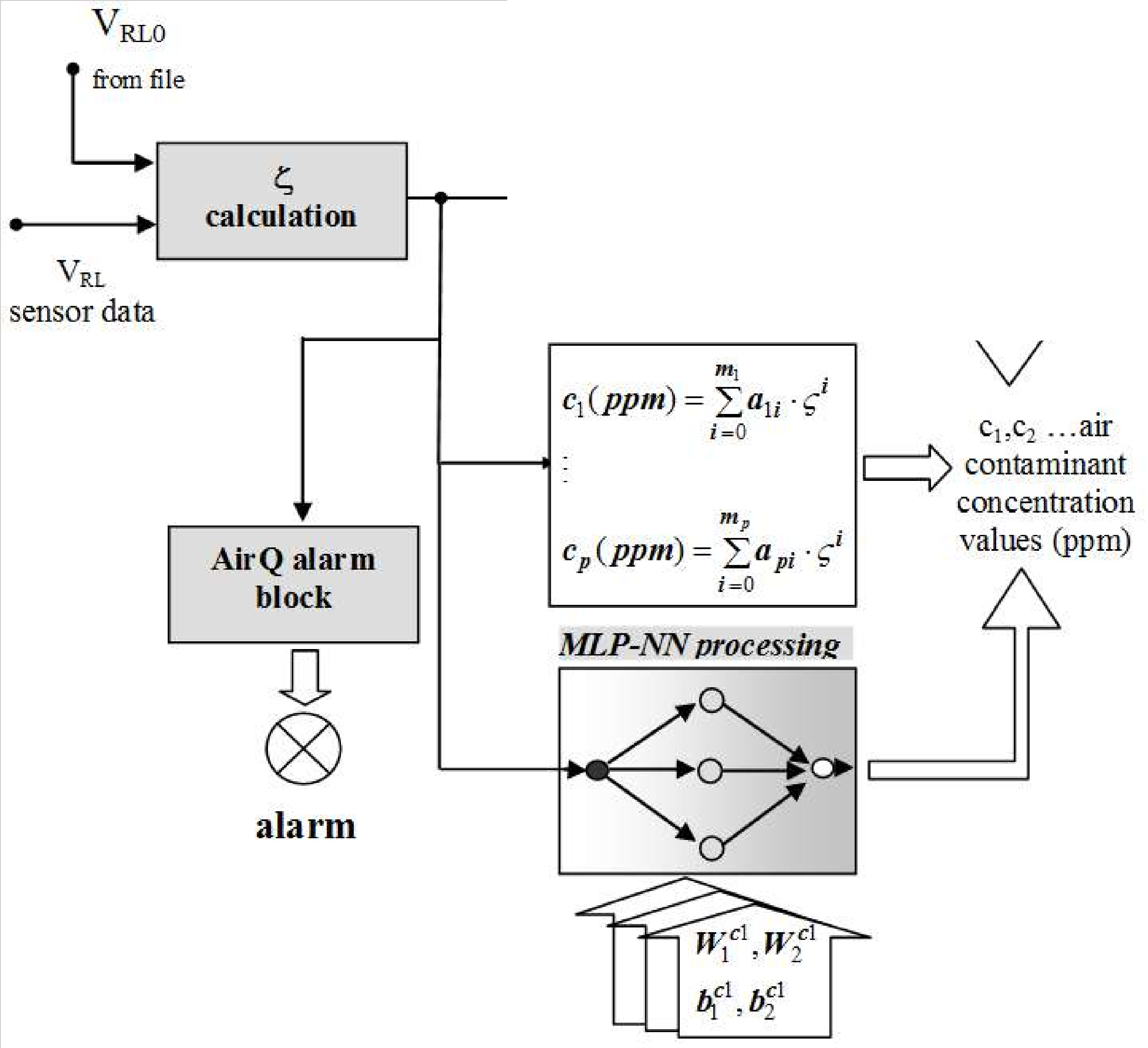

Figure 4.

Block diagram of the hybrid data processing scheme that was used to evaluate contaminants' air concentrations.

To test the performance of the proposed modeling scheme, a set of coefficient values (ζ), contained in the interval between 0.15 and 1 (no pollution), and the correspondent values of air contaminants' concentrations obtained from TGS800 sensitivity curves for methane, carbon monoxide, isobutane, hydrogen and ethanol, were considered. The calculation of polynomial coefficients, a_{1i}, a_{2i}, ... a_{pi}, is based on LS linear fit function (Givens method) that is implemented in LabVIEW. The calculated polynomial coefficients values that correspond to TGS800 sensitivity curves, such as the ones represented in , are stored in a memory and then used to perform the evaluation of air contaminants' concentrations.

The used neural processing blocks (NPB_i) is related with the inverse modeling [ ] of gas sensor multivariable nonlinear characteristics, which are strongly dependent on temperature and humidity but also influenced by the concentration of other gases of the analyzed gas mixture. Based on the designed NPB_i, a digital read-out of the gases concentration with temperature and compe

Regarding the NPB_i, two inputs one output multilayer perceptron neura normalization blocks and denormalization blocks used for ANN input a

The NPB_i's internal parameters (weights and biases) are off-line calculat system calibration phase. They are voltage values (V_{GSi}) acquired from (C_{Gi}), and different temperature (T_p) and relative humidities (RH_i) val

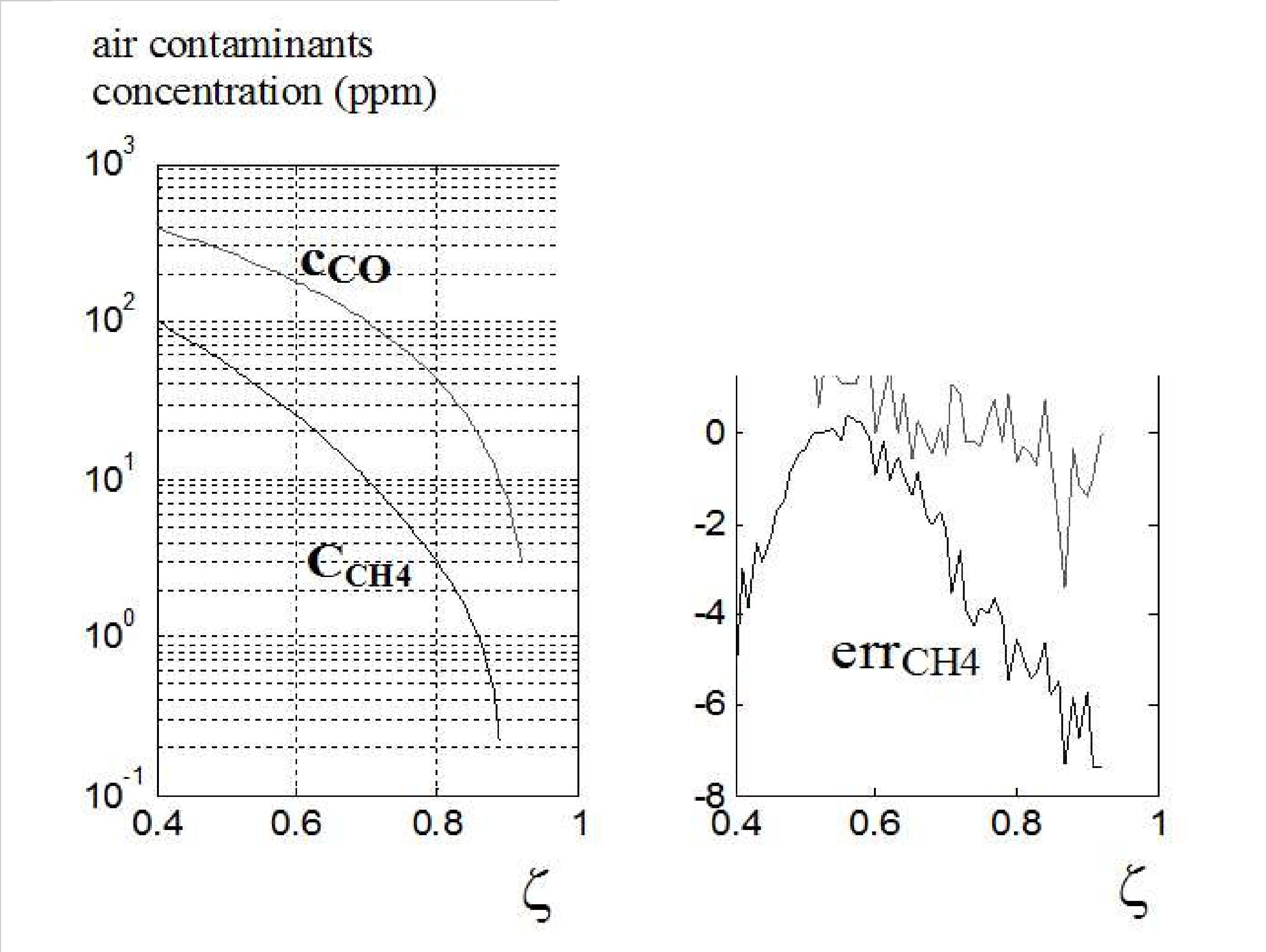

Figure 5.

Polynomial approximation of air contaminants curves (CO and methane case) and polynomial approximation error (err_{CO}, err_{CH_4})

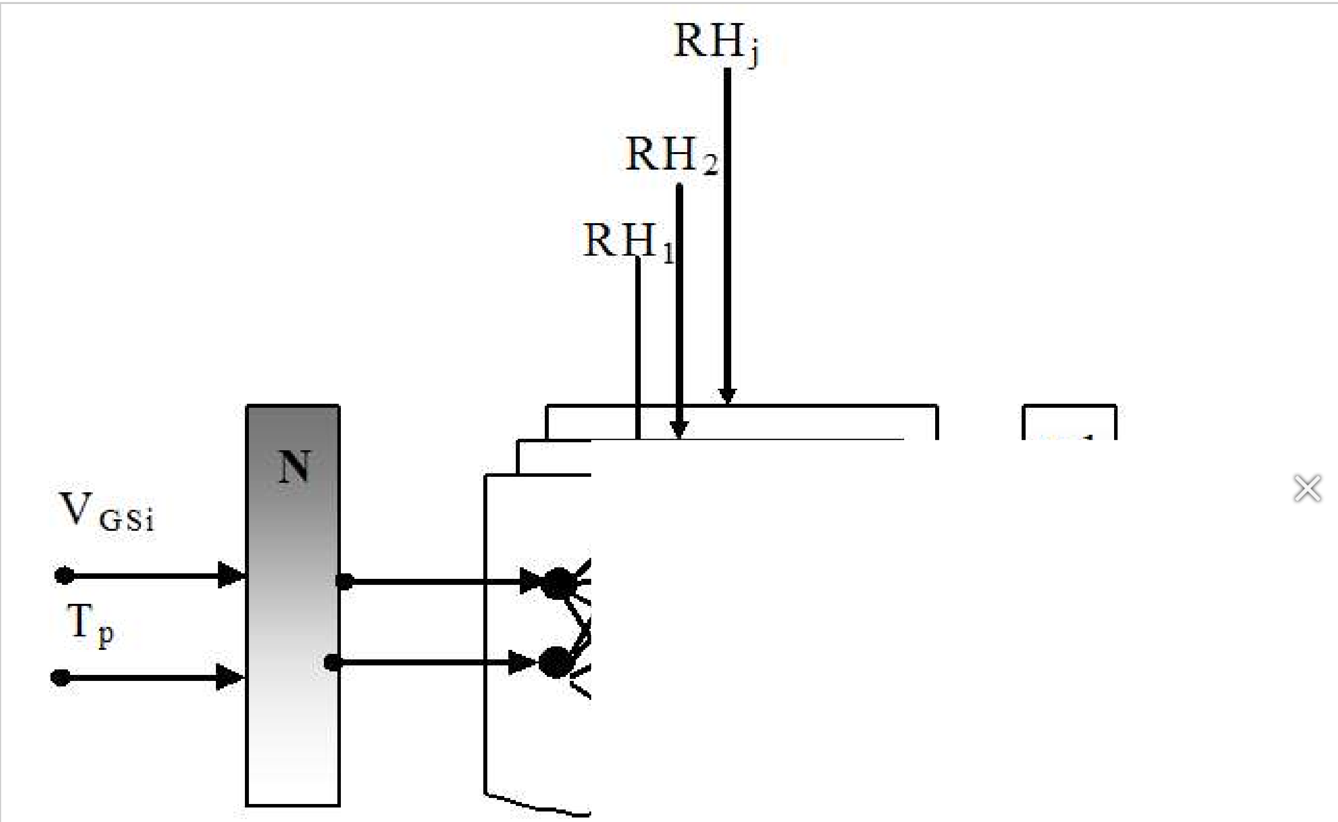

Figure 6.

NPB_i architecture (N, N^{-1}: normalization anc
temperature and humidity compensated valu
V_{GSi}: input voltage value on the GS_i channel)

The neural network algorithm developed in MATLAB software calculat
55%, 65%}. The NPB_i input is the normalized voltage associated with ea
temperature compensated gas concentration (C_{Gi}). The NPBi normalize

$$V_{GSi}^{N} = \cdot$$

E9

where $V1_S$ represents the gas sensor normalization factor (GS_i voltage supply=+10V in the present case).

Because GSi characteristics depend on humidity, an accurate measurement of the gas concentration is provided using different $NPB_i|_{RH}$ whose weights and biases are calculated using the data obtained for predefined relative humidity conditions (RH=45%, 55% and 65%) and by the interpolation method presented in [ ].

The number of NPBi's layers is three. The hidden layers have 2 to 5 tansignoid (tansig(x)) neurons, and the output layer has 1 linear (l(x)) neuron. The implemented tansig(x) calculates its output according to

$$\tan sig(x) = \frac{2}{1+\exp(-2x)} - 1$$

E10

which leads to a reduction of the computational load.

Two criteria for NPBi design were considered, the type and the number of neurons on the hidden layer, both determining the capabilities of the NPBi to adapt to a given characteristic. Different neuron nonlinear activation functions require different memory space and processing capabilities from the hardware platform.

To reduce the weights and biases in vector sizes, several simulation tests concerning the number of neurons for a required NPB_i performance, expressed by a modeling error, were performed. ANNs with a higher number of neurons increase processing load and, moreover, require larger memories to store weights and biases matrices. The results of these simulations are particularly important when embedded systems are used to implement the neural processing architecture (e.g. 512k EEPROM in the IPμ8930 case).

For the particular case of the CO measuring channel, the training set includes, as target, fifteen CO concentration values uniformly distributed in the 30 to 300ppm interval. The input values are the voltage values acquired from the TGS203 CO concentration measuring channel corresponding to the above-mentioned concentrations. The measured temperature in the testing chamber was T_p[°C]=10×p, p={1,2,3,4,5} and the relative humidity RH=35%. The Levenberg Marquardt algorithm [ ] was used to calculate the weights and biases (W_{NPBi}, B_{NPBi}) of the neural network. Imposing a sum square error stop condition SSE=0.01, and for neural networks characterized by 4, 5 or 6 hidden neurons, different measuring channel modeling error characteristics (e_{CGsi}) were obtained ( ). The modeling error is defined by:

$$e_{CGsi} = \frac{C_{CGsi} - C_{CGsi}^{NPB}}{FS} \times 100$$

E11

where FS represents the measurement range, CCGsi is the experimental used gas concentration (e.g. carbon monoxide concentration) expressed in ppm, and C_{CGsi}^{NPB} the concentration of gas calculated by the corresponding neural processing module.

Since the used gas sensors characteristic depends on temperature, a study related with the CO channel modeling error (e_{CO}) versus temperature was carried out ( ).

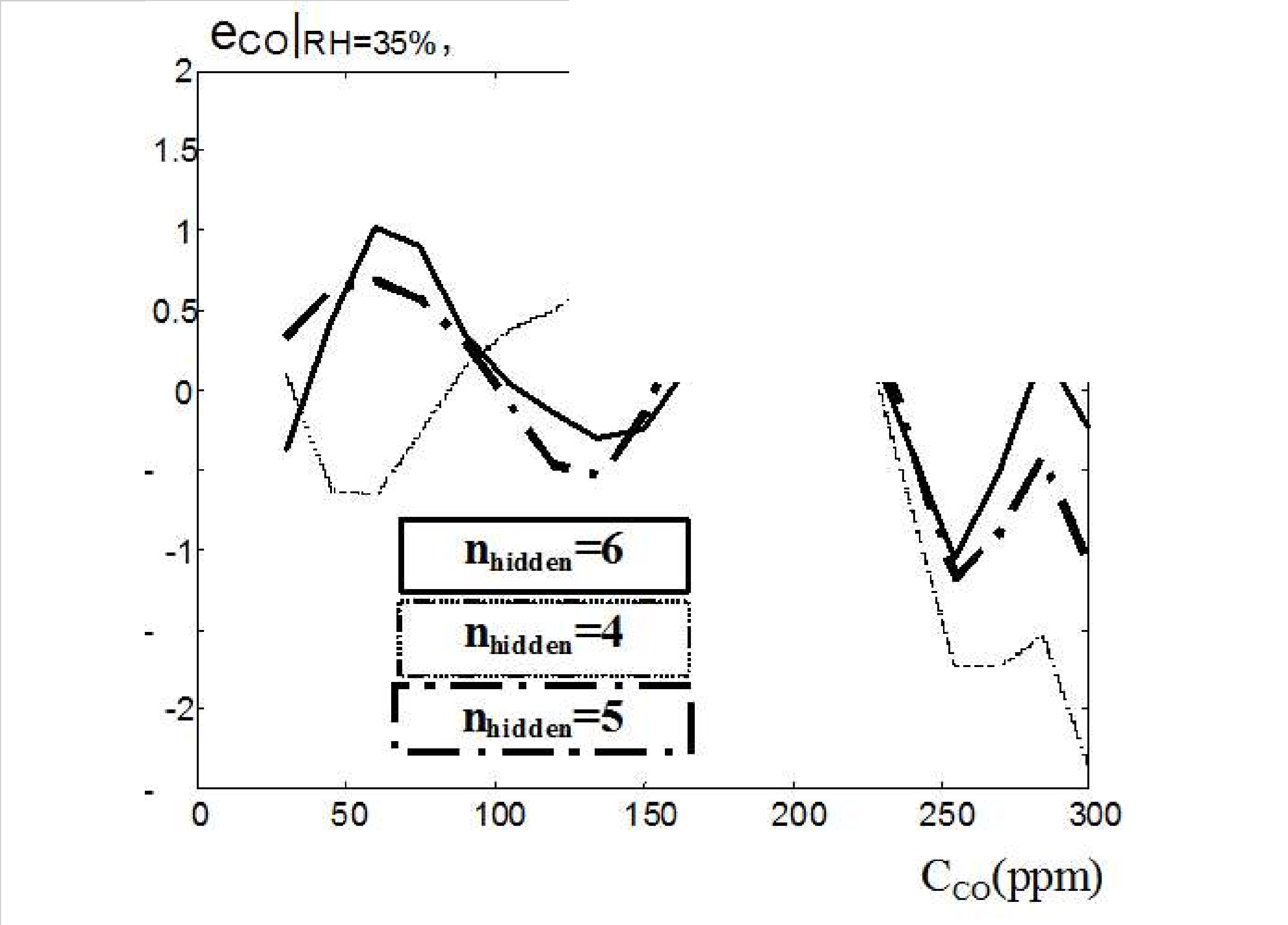

Figure 7.

The modeling error versus concentration for different NPB_{CO} architectures (T=10°C)

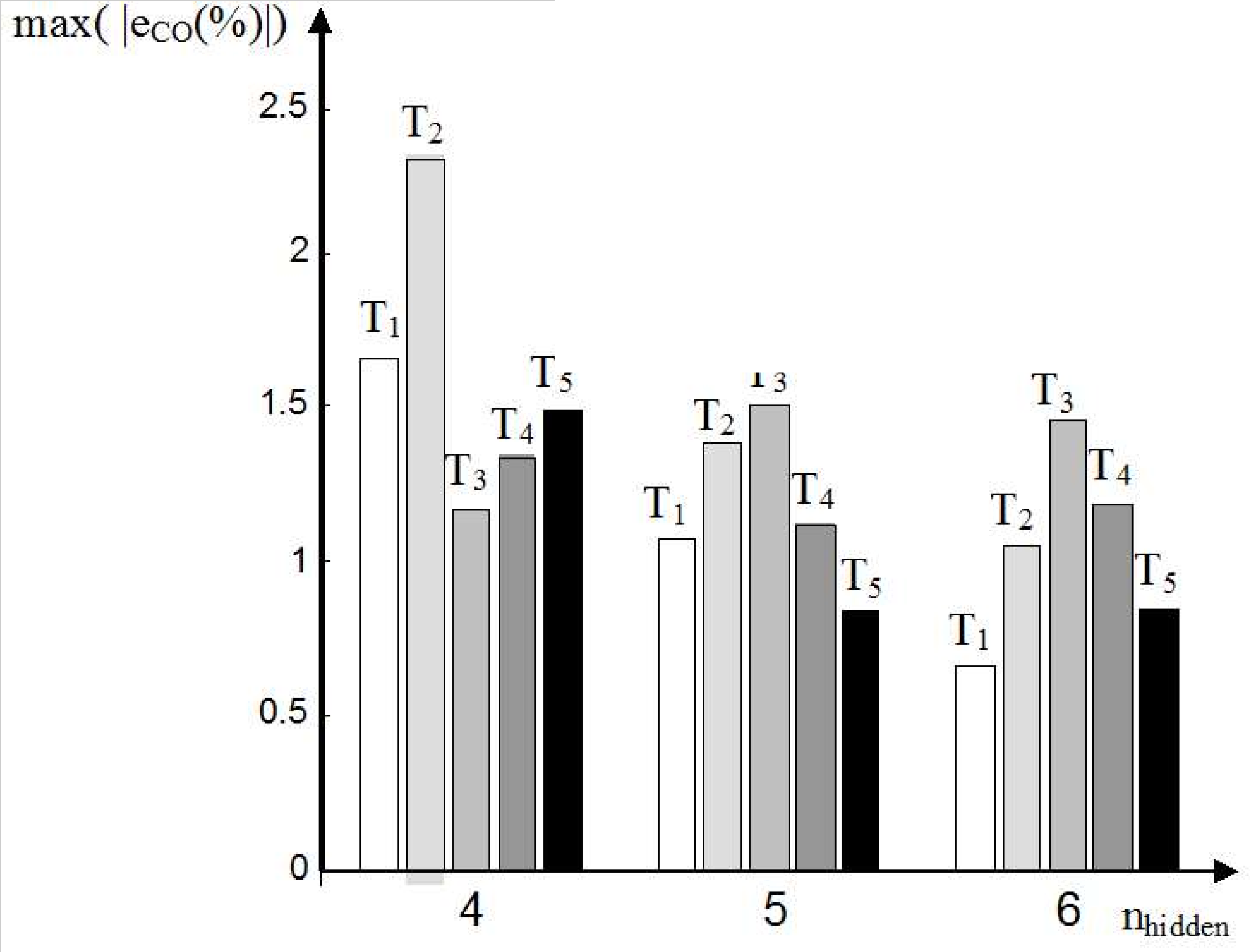

Figure 8.

The maximum inverse modeling error for different NPB_{CO} architectures (n_{hidden}={4, 5, 6}) and different temperatures T_p=10 p ºC

Being humidity an influence quantity, different values of the relative humidity lead to different primary gas selectivity characteristics and hence to different gas concentration measurement accuracies. Thus, experimental data obtained for three different values of relative humidity, RH_1=35%, RH_2=65% and RH_3=95%, and five values of temperatures included in the I_T=[10;50]ºC were considered. The imposed gas concentrations for measurement system testing were: 10 values of methane concentration distributed in the I_{CM}=[500;5000] ppm interval, 15 values of carbon monoxide concentration I_{CCO}=[30;300] ppm, and 15 values of solvent vapors (Ethanol vapors) concentration, C_{SV}=[50;5000] ppm.

Based on the GS_i voltages for the considered gases concentrations, and taking into account temperature and humidity, three sets of weights and biases (35%, 65% and 95% relative humidity) were calculated for carbon monoxide, methane and solvent vapor measurement channels.

4. Smart sensing networks for air quality assessment

Gas sensors networks provide a promising mechanism for mining information from the monitored areas. Point-to-point and multipoint wireless network architectures, including sensing nodes, materialize the implementations in the air quality monitoring for indoor and outdoor conditions.


ENGLAND
London
Birmingham
FRANCE
PYRENEES
Madrid
Barcelona

A. Point-to-point network architecture
Different architectures were developed by the authors, one of them base
(AIR-Q VMS) that joins hardware and software components to assure h
the mobile indoor air quality monitor system is presented in .

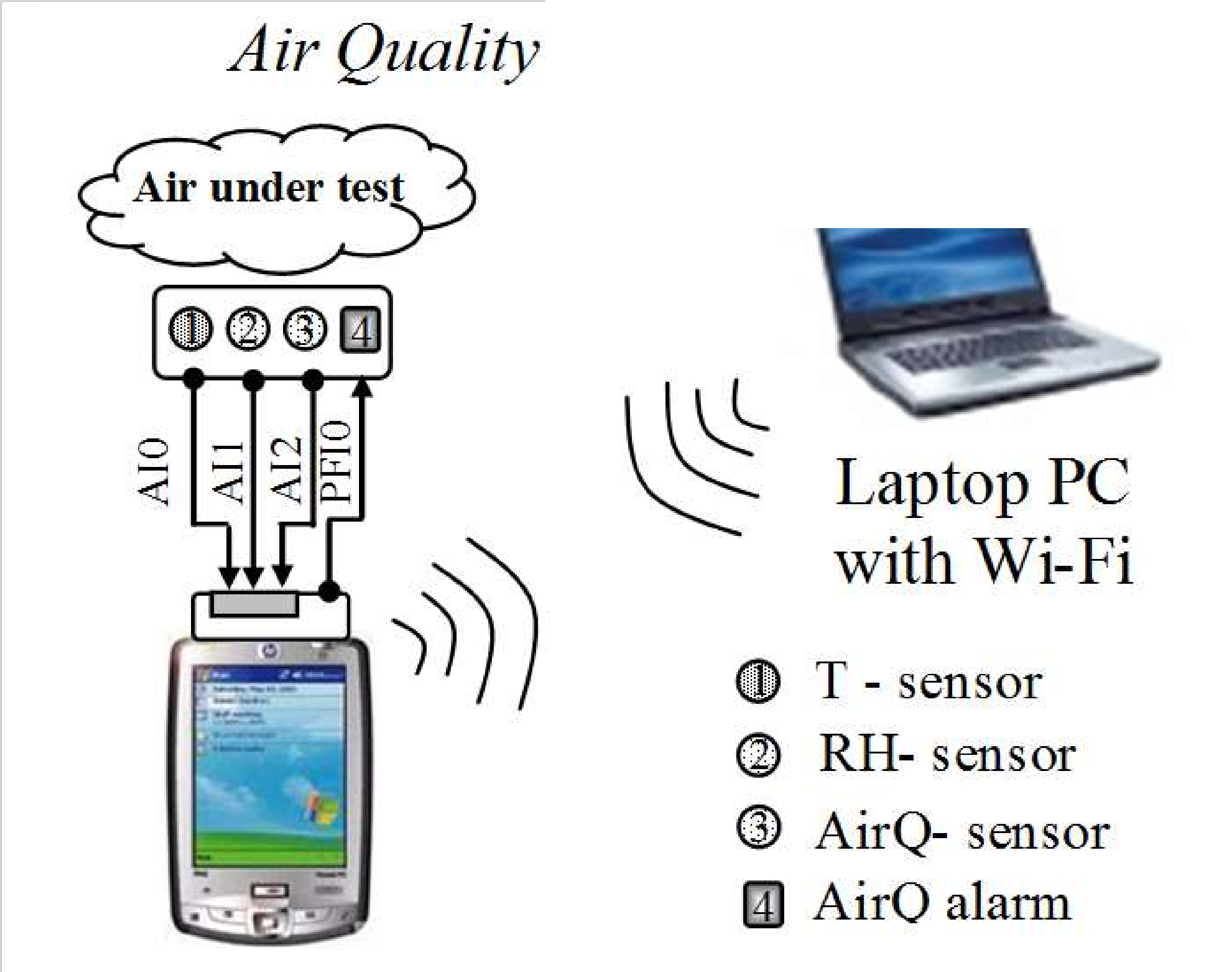

Figure 9.

Mobile Air Quality system based on a PDA with a compact flash (CF) multifunction I/O board

The sensing node includes sensors (temperature, relative humidity, and air quality), conditioning circuits, a compact flash data acquisition device DAQ (NI CF-6004) and a PDA with wireless communication capabilities (Wi-Fi or Bluetooth). A point-to-point connection between the measurement node and an advanced processing and communication unit (a PC) permits to deliver the air quality data from the sensing node to the PC and to receive information, such as alarm thresholds, that is used to implement alarm mechanisms in the PDA. The acquired data is processed by the PDA and the results are displayed by the PDA GUI.

Considering the cost of the implementation of the air quality sensing node based on a DAQ board plugged to a PDA, and also taking into account the evolution of the area of pervasive computing,, the authors decided to develop air quality monitoring systems based on smart phones and Bluetooth enabled smart sensors. The implemented architecture is presented in .

Figure 10.

Air quality virtual measuring system's architecture based on a smart sensing node (SN) with Bluetooth communication capabilities, and on a smart phone

The smart sensors indicated in are specialized for temperature, air quality and air quality index measurement [ ]. When monitoring large spaces, the number of sensing nodes increases, which means that point-to-multipoint architectures must be considered.

B. Point-to-multipoint Bluetooth architecture and embedded smart phone software
An implementation of a point-to-multipoint network architecture that uses Bluetooth compatible smart sensing nodes is presented in . The sensing nodes provide information about the level of relative humidity, temperature, and air contaminants (e.g. undesired odours that can trigger respiratory disorders). As computation units and human machine interface are included a laptop PC that works as the system server, a touch panel computer (TPC) and a smart phone (SP).

The implemented Bluetooth scatter net architecture assures the remote monitoring of the sensing nodes and data communication between the mobile device and smart sensor nodes. The hardware component of the system includes: sensors and conditioning circuits, a data acquisition device Bluetooth enabled (e.g. BlueSentry from Grid Connect), a smart phone with Bluetooth interface (e.g. N70 from Nokia), a situated display (NI TPC2106) Bluetooth compatible through a RS232-to-Bluetooth bridge, and a data communication, data processing and data storage unit (laptop PC).

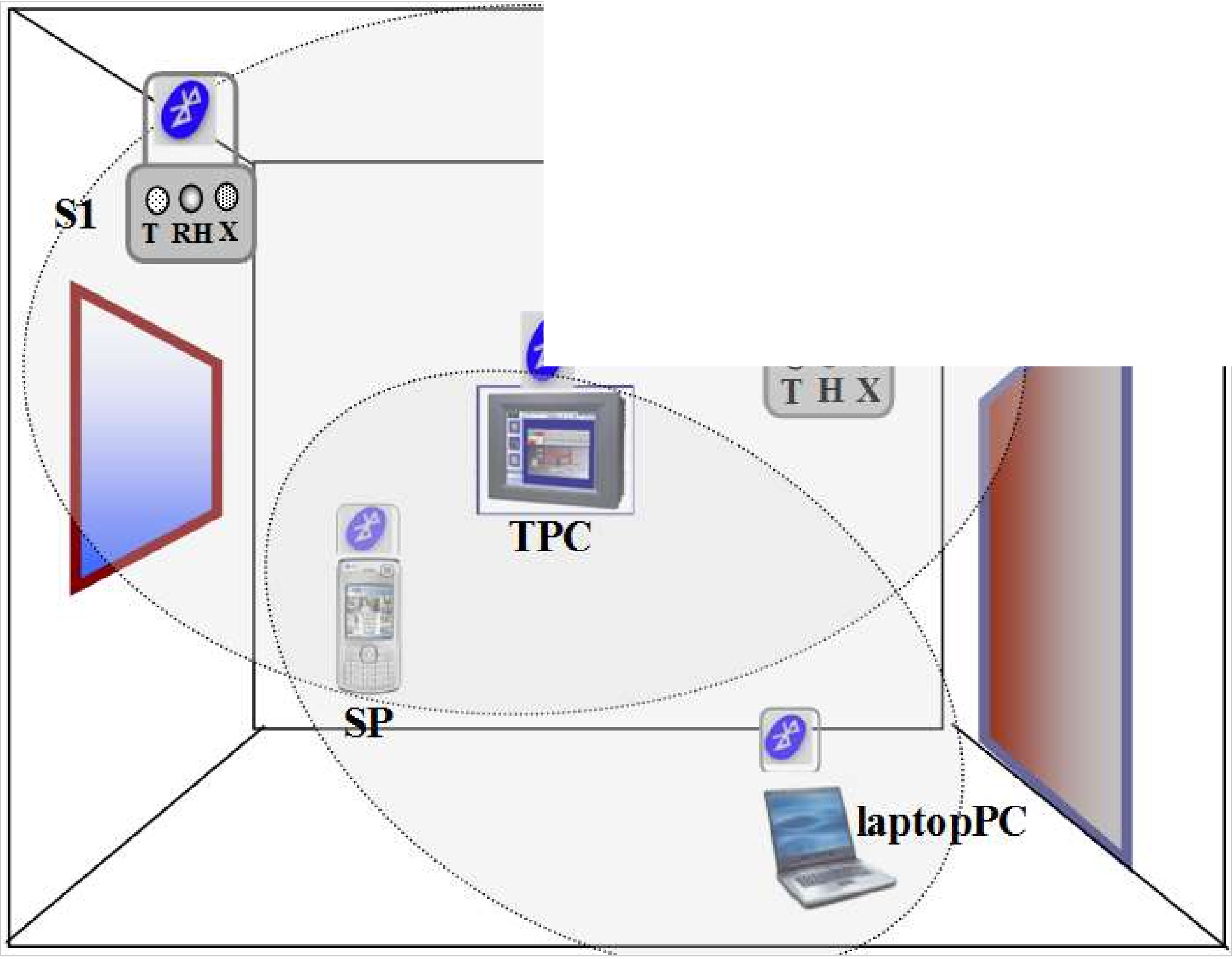

Figure 11.

Distributed air quality measurement architecture associated with respiratory distress triggering factors monitoring based on Bluetooth networking protocol (S1 and S2 are the sensing nodes characterized by T-temperature, H – relative humidity and X- air quality index measurement channel, TPC- touch panel computer, SP- smart phone)

The software technologies used to develop the applications for the smart phone running Symbian OS and for the TPC running Windows CE OS, were Java2Me and LabVIEW. The application embedded in the smart phone was named SmartSense Mobile. AirQUbicomp is the application developed using LabVIEW 8.6 Touch Panel Module for the TPC. This application provides the information about indoor air quality.

The SmartSense application has the ability to identify the active smart sensing nodes, to establish a connection via Bluetooth with the nodes, to control the on/off state of the air quality index sensor (XairQ-sensor), and to collect voltage samples from relative humidity, temperature and air quality measuring channels of each node in single-shot mode or in continuous mode.

SmartSense also assures the transfer of the indoor air quality values calculated and stored in the smart phone memory extension to the laptop PC through Bluetooth synchronization.

After node(s) selection, the operator can choose between the "one samp
in order to test the normal functioning of the sensing node or to verify t
broadband pollution) during the system setup.

Working in continuous acquisition mode, the smart phone application p
thresholds previously stored in the SmartSense Mobile configuration fil
files received through Bluetooth from the PC that runs a SmartAdmin a
to 60 min interval were considered. These values are adapted to the sma
temperature, humidity and XairQ index measurement. During continu
converted into physical values by the SmartSense Mobile application an
phone whose number was written in the SmartSense configuration file.

The continuous acquisition and data conversion software modules work
inform that indoor air conditions are critical. The used threshold values

Th	
	RH[%]
thmin	30
thmax	50

Table 1.

Threshold values for relative humidity, temp
likelihood of asthma attack.

During visual or acoustic signalling, a set of useful recommendations related to indoor air factors values and the actions necessary to change the indoor air conditions from critical to normal are available through the smart phone GUI.

The AirQUbicomp application is designed to continuously monitor the air quality, generating visual and acoustic alarms according to the imposed thresholds. Active interaction with the touch panel computer is permitted after identification of the user through a numeric password. After identification, the user can modify the thresholds related to asthma or can define data logging elements such as the time between readings and the monitoring period (DLog TAB in). The values of temperature, air quality and air quality index as well as the alarms LEDs (AirQ Alarm) are part of the T-RH-XAirQ software TAB. In the GUI associated with AirQUbicomp is presented.

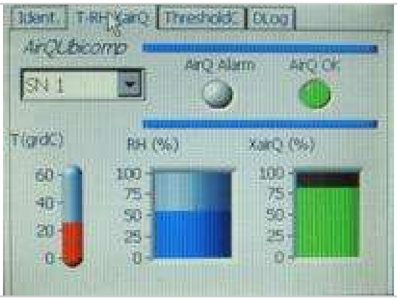

Figure 12.

AirQUbicomp GUI

Using the developed SmartSense Mobile application different tests associated with indoor air quality monitoring were carried out. The data stored in the Nokia N70, is wireless transferred to the database implemented in the laptop PC. Some data related with continuous measurement of the asthma or COPD attack triggering factors are presented in .

In the relative humidity is in the limit of automatic alarm generation (RH>50%) while temperature and air quality are inside the interval values associated with “no asthma or COPD attack conditions”.

In can be observed low levels of the XairQ index when the measurement session started. Based on the information displayed, the user acted to improve the air quality (e.g. by opening the window). The air quality started to improve and, at the same time, room’s temperature and humidity change significantly.

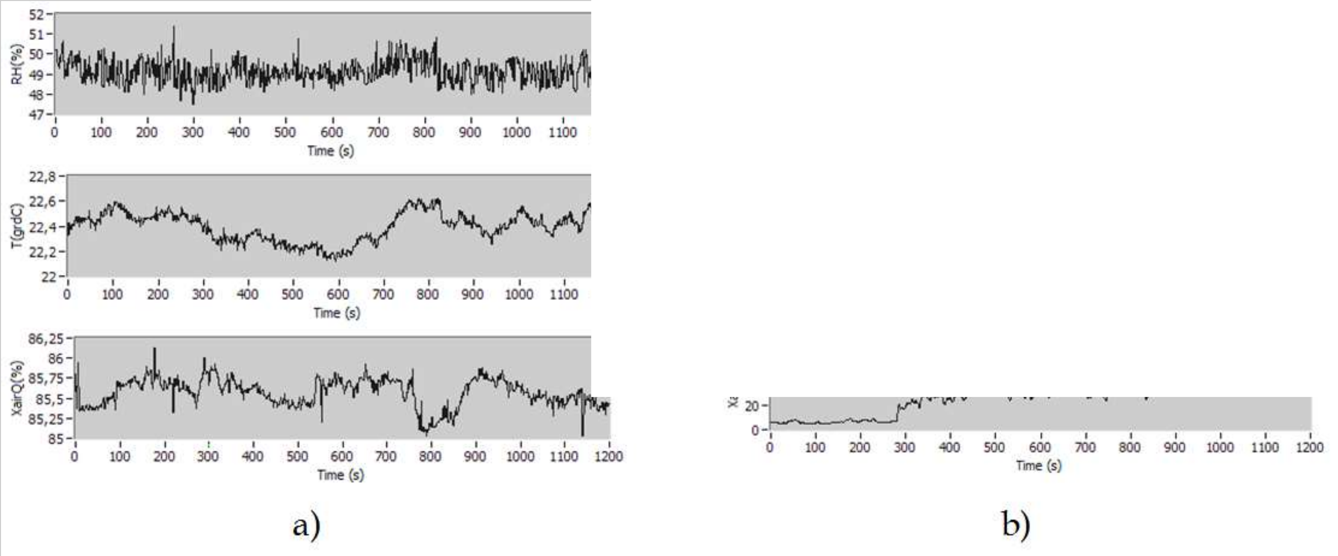

Figure 13.

S1 node monitoring of respiratory distress triggering factors

In order to find correlations between the air quality and the values of physiological parameters, such as oxygen saturation (SpO2) and heart rate (HR), a digital pulse oxymeter and electrocardiograph apparatus ECG Medlab P-OX 100 was used for testing purposes. presents the results of SpO2 and HR for two volunteers, with and without respiratory distress history (RD-N, RD-Y). The physiological values were measured in the same room and for the volunteers seated on a chair.

Analyzing the data from , one can notice that in case of the healthy individual (RD-N), values of XairQ lower than 80% and of RH near 50% do not induce changes in HR and SpO2, while a significant increase in the HR of RD-Y is felt.

Sensor node	T (°C)	RH (%)	XairQ(%)	RD-N		RD-Y	
				HR	SpO2	HR	SpO2
S1	17.2	47.4	62.7	72	98	96	92
S2	17.8	44.2	69.6				

Table 2.

S1 node: air quality and physiological parameter values for two volunteers, with and without respiratory distress history

Nowadays, smart phones are provided with operating systems, such as Android OS and iOS, which make the implementation of complex software modules easier and faster. The authors have been working to develop an AirQ Android OS application for a multichannel sensing node. The graphical interface of the implemented application is presented in .

The AirQ dashboard includes elements related with respiration activity (respiration rate). The data logging procedure is done using a smart phone embedded database that can synchronize with Web-based information system database through Wi-Fi or 3G/UMTS communication protocol.

Figure 14.

AirQ graphical interface implemented in the AndroidOS smart phone

5. Conclusion

The quality of life of pulmonary patients greatly depends on the quality of the air they breathe. The identification of the indoor air associated with pathophysiology of COPD and asthma disease is crucial for the primary-prevention strategy. In the preceding paragraphs the authors summarize the main elements of a distributed smart sensing network for indoor air quality assessment. Regarding sensing nodes and signal conditioning, two possible solutions were presented. One based on semiconductor heated sensors and another based on three electrodes' cells. For data processing purposes, a hybrid solution based on polynomial and artificial neural networks modelling is presented. The last part of the chapter includes possible solutions for indoor air quality smart sensing networks.

Download for free

Share

More

PRINT CHAPTER

How to cite and reference

Link to this chapter Copy to clipboard

https://www.intechopen.com/books/chemistry-emission-control-radioactive-pollution-and-indoor-air-quality/distributed-smart-sensing-systems-for-in

Cite this chapter Copy to clipboard

Octavian Postolache, Jose Miguel Pereira, Pedro S
Distributed Smart Sensing Systems for Indoor Mo
Chemistry, Emission Control, Radioactive Polluti
DOI: 10.5772/16929. Available from: https://www.
radioactive-pollution-and-indoor-air-quality/dist
respiratory-distress-triggering-factors

Chapter statistics

Related Content

This Book

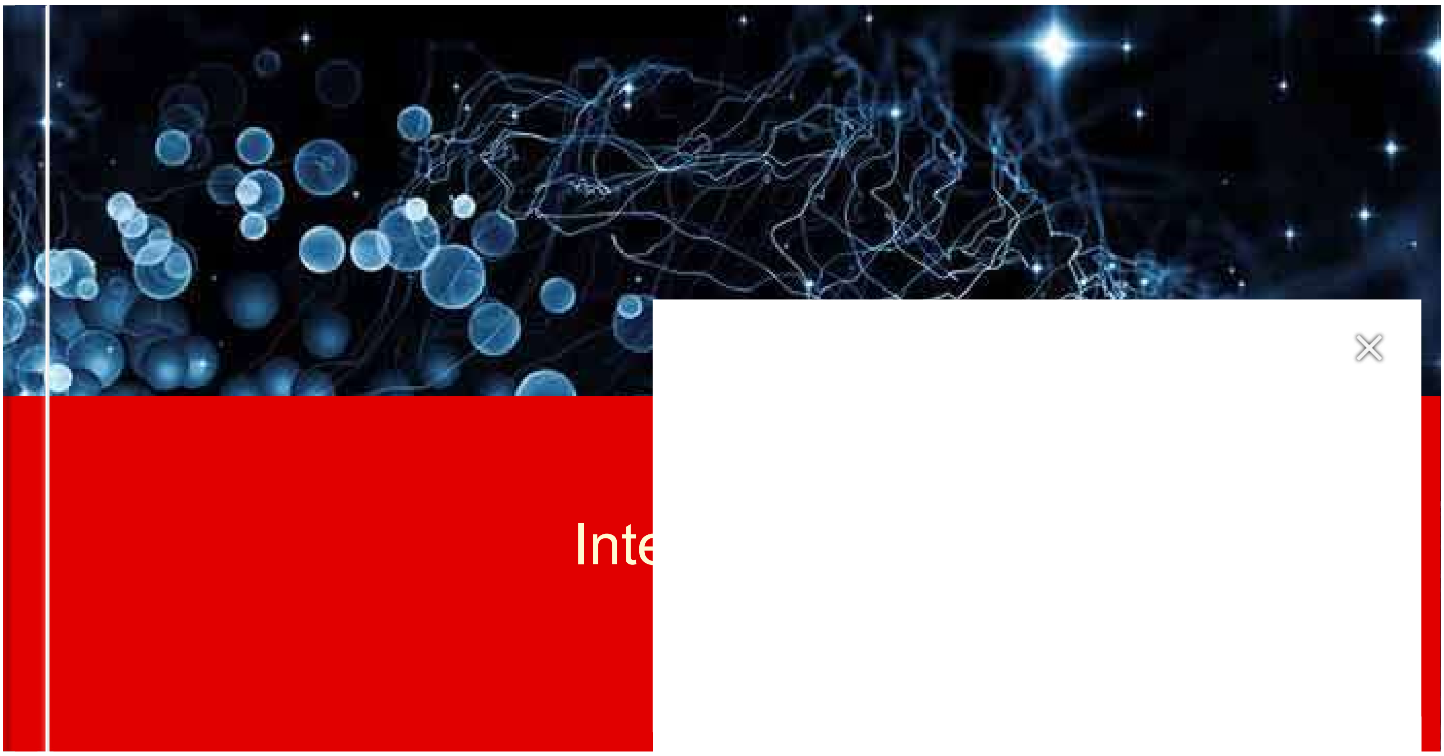

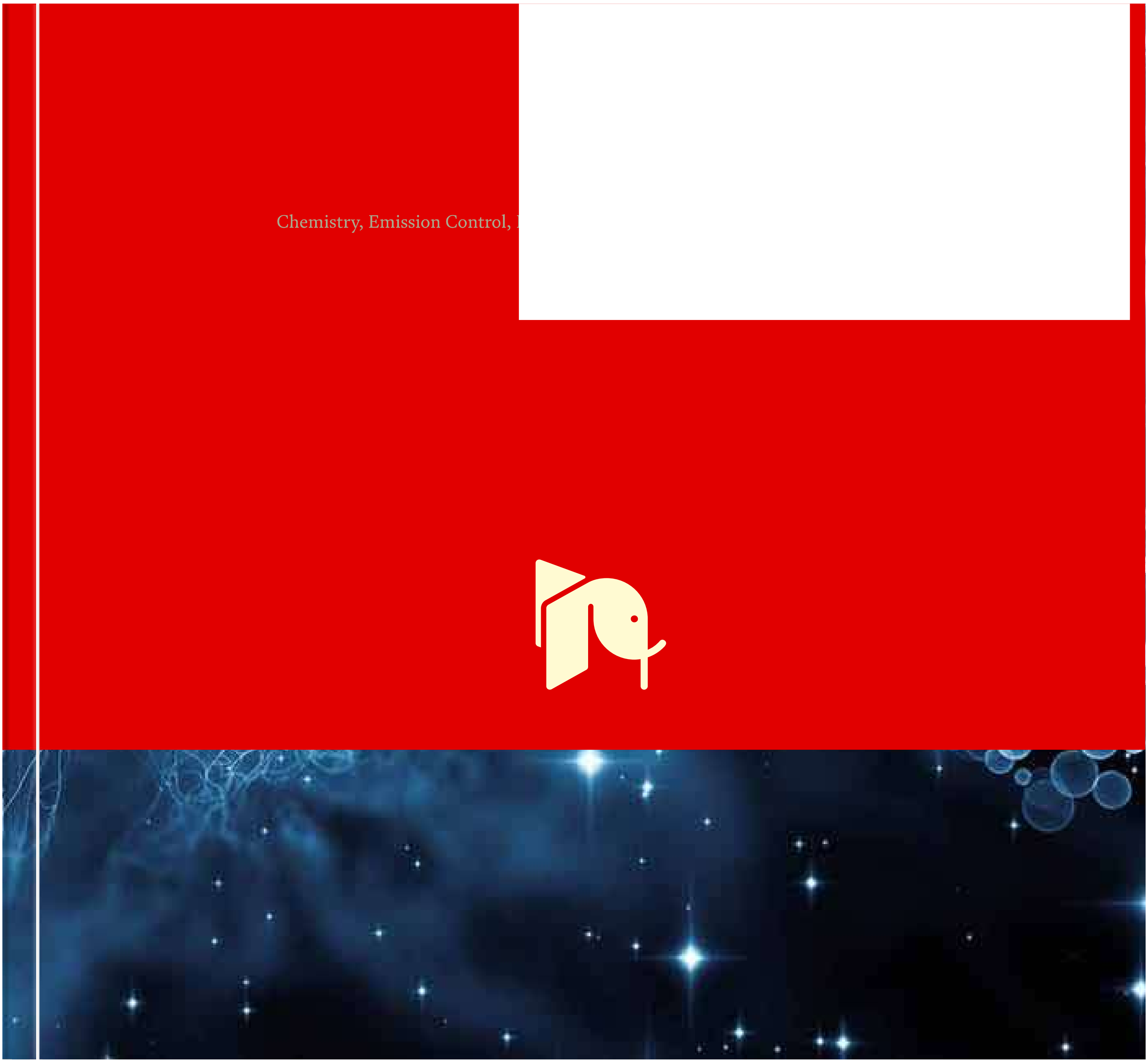

An Exposure Model for Identifying Health Risk due to Environmental Microbial Contamination in the Healthcare Setting

By M.D. Larranaga, Enusha Karunasena, H.W. Holder, Eric D. Althouse and David Straus

Chemistry, Emission Control, Radioactive Pollution and Indoor Air Quality

Edited by

Related Book

Planning Air Pollution Monitoring Networks in Industrial Areas by Means

By Mauro Rotatori, Rosamaria Salvatori and R

Air Quality Monitoring, Assessment and Mana

Edited by

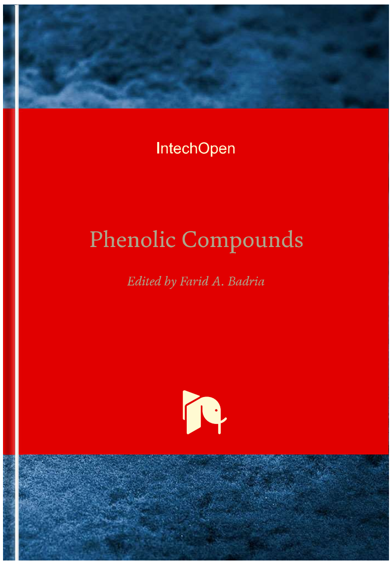

Phenolic Compounds

Edited by Farid A. Badria

Open for chapter submissions

Herbs and Spices - New Processing Technologies

Edited by Rabia Shabir Ahmad

Open for chapter submissions

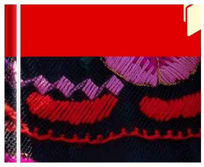

Heritage - Ne

Edited by Daniela

Open for chapt

Book Subject Areas

Physical Sciences, Engineering and Technology

Chemistry

Computer and Information Science

Earth and Planetary Sciences

Engineering

Materials Science

Mathematics

Nanotechnology and Nanomaterials

Physics

Robotics

Technology

More ›

Life Sciences

Agricultural and Biological Sciences

Biochemistry, Genetics and Molecular Biolc

Environmental Sciences

Immunology and Microbiology

Neuroscience

More >

Health Sciences

Medicine

Pharmacology, Toxicology and Pharmaceutical Science

Veterinary Medicine and Science

Social Sciences and Humanities

Business, Management and Economics

Psychology

Social Sciences

>

Home

News

Contact

Careers

About

Our Authors and Editors

Scientific Advisors

Team

Events

Advertising

Partnerships

Publish

About Open Access

How it works

OA Publishing Fees

Open Access funding

Peer Reviewing

Editorial Policies

Headquarters
IntechOpen Limited
5 Princes Gate Court,
London, SW7 2QJ,
UNITED KINGDOM

Phone: +44 20 8089 5702

Search

AUTHOR PANEL SIGN IN

Terms and Conditions | Privacy Policy | Customer Complaints